Polymer Chemistry

ROYAL SOCIETY OF CHEMISTRY

COMMUNICATION

View Article Online
View Journal | View Issue

Cite this: *Polym. Chem.*, 2020, **11**, 7481

Received 15th September 2020,
Accepted 22nd November 2020

DOI: 10.1039/d0py01329c

rsc.li/polymers

Confined supramolecular polymers in water with exceptional stability, photoluminescence and chiroptical properties†

Anurag Mukherjee, Deep Sankar Pal, Haridas Kar and Suhrit Ghosh *

This communication reveals the synthesis of lipid-encased chiral supramolecular polymer nanorods (SPNRs) in water from a hydrophobic naphthalene-diimide derivative by the nanoprecipitation technique. The as-prepared SPNRs exhibit exceptional thermal stability (T_m > 90 °C), excellent photoluminescence (Φ > 0.5 compared to <0.01 of the monomeric dye) and circularly polarized luminescence with a very high chiral dissymmetry factor (g_{lum}) of ~0.8 × 10^{-1} which has rarely been reported for any supramolecular polymer.

Supramolecular polymers of π-systems have emerged as an important inter-disciplinary research area in the past two decades.[1] While exploring them as functional materials continues to be an active area,[2] recently the focus has been shifted to pathway complexity and controlled/living supramolecular polymerization.[3] In majority of examples,[1–3] supramolecular polymerization has been shown in less-polarizable solvents, wherein H-bonding and π-stacking display prominent effects. More recently their aqueous supramolecular assembly has also been studied with great interest,[4] especially due to their potential application as supramolecular biomaterials.[5] Although structurally diverse π-systems have been tested for supramolecular polymerization,[1–4] most of them exhibit fluorescence quenching in the polymeric state, whether in hydrocarbon or in water, which limits the scope of their wider applications in biology or materials science. Recently we have reported cooperative supramolecular polymerization of a core-substituted naphthalene-diimide (NDI) derivative (NDI-1, Scheme 1) in decane with a highly fluorescent chiral nanostructure and circularly polarized luminescence (CPL).[6] Inspired by such excellent chirotopic and optical properties, we recognized that the scope of this system for biological applications would be much broader if such properties can be realized in aqueous media. Instead of designing a new water-soluble derivative of the same chromophore (which invariably comes with the uncertainty of realizing similar photophysical effects), we have dispersed the hydrophobic NDI-1 itself in water with the aid of a commercially available polyethylene-glycol attached phospholipid (DSPE-PEG, Scheme 1). In a broader sense, conceptually similar strategies are well-established for the preparation of nanoparticles from conjugated polymers[7] in water, which show promising results for various biological applications.[8] Despite growing interest in this field, such examples of particulate colloids[9] derived from supramolecular polymers are limited to only a handful of systems.[10–12] In this communication we report the synthesis of lipid-encased supramolecular polymer nanorods (SPNRs) in water from hydrophobic NDI-1 with tunable size and illustrate remarkable confinement effects on the thermodynamic stability, photoluminescence and chiroptical properties.

DSPE-PEG lipid encapsulated SPNRs of NDI-1 were synthesized by a modified nanoprecipitation method (Scheme 2a).[10a,13] A solution of DSPE-PEG (4.0 mg) and NDI-1 (1.0 mg) in THF was injected into excess water, sonicated for a few minutes and allowed to stir overnight at 50 °C to evaporate

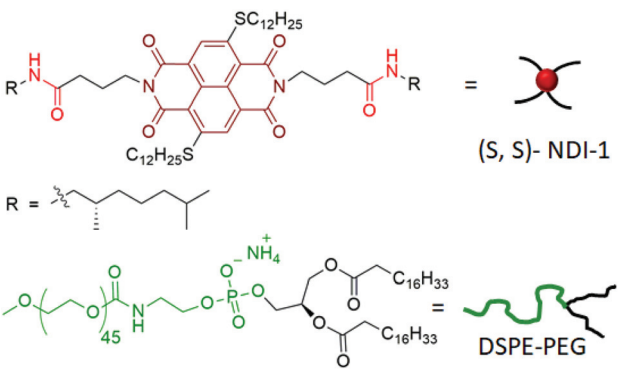

Scheme 1 Structures of (*S*, *S*) NDI-1 and DSPE-PEG.

School of Applied and Interdisciplinary Sciences, Indian Association for the Cultivation of Science, 2A and 2B Raja S. C. Mullick Road, Kolkata, 700032, India. E-mail: psusg2@iacs.res.in

†Electronic supplementary information (ESI) available: Experimental detail and additional characterization data for supramolecular polymer nanorods. See DOI: 10.1039/d0py01329c

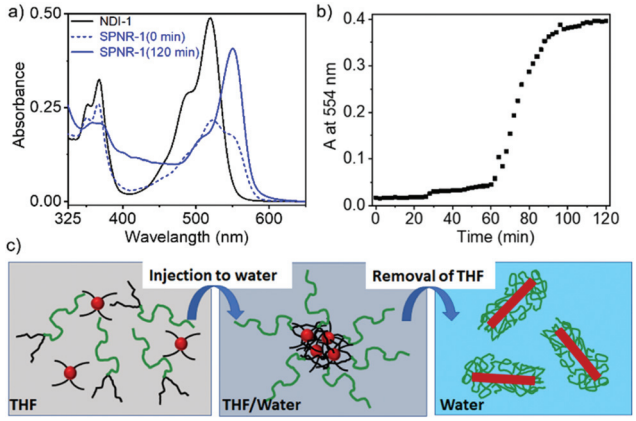

Scheme 2 (a) UV/Vis spectra (l = 1.0 cm) of monomeric NDI-1 in THF (c = 0.35 mM), the sample obtained just after injecting NDI-1 (0.1 mg) + DSPE-PEG (4 mg) solution in THF (300 μL) into water (2000 μL) (0 min) and the sample two hours after being kept at 50 °C in the cuvette without a lid; (b) change in absorption intensity at 554 nm as a function of time when the THF solution was injected into water and left at 50 °C with an open lid; and (c) schematic representation of the possible growth process during the synthesis of SPNRs.

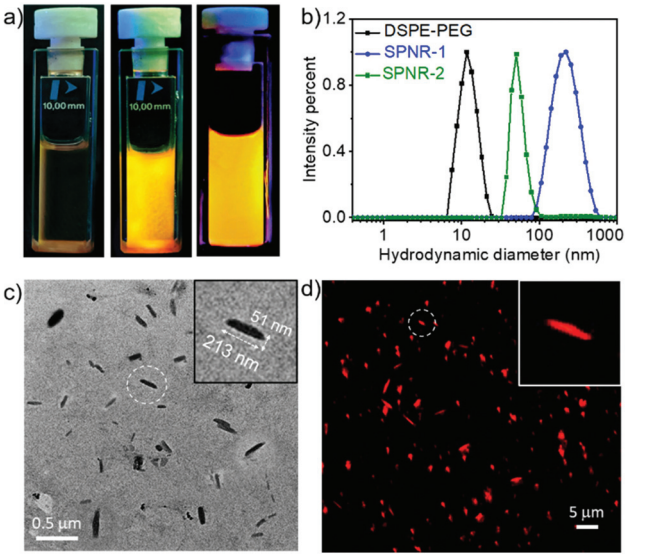

Fig. 1 (a) Images in the left – monomeric NDI-1 solution in THF (c = 0.35 mM), middle – SPNR-1 (concentration of NDI-1 = 0.34 mM) and right – SPNR-2 (concentration of NDI-1 = 0.031 mM) under a UV-lamp; (b) size distribution of aqueous aggregates of DSPE-PEG (c = 2 mg mL^{-1}), SPNR-1 and SPNR-2 from DLS; (c and d) TEM and fluorescence microscopy images of SPNR-1. Insets show zoomed images from the selected region marked with a circle. The fluorescence microscopy image does not represent the actual emission colour (a) as the image was acquired by setting the red filter which cuts off any light outside its wavelength window.

THF producing a homogeneous dispersion. Thereafter the solution was dialysed and then filtered to ensure removal of any residual THF or smaller particles. The homogeneous dispersion, labelled as SPNR-1, appeared highly fluorescent under a UV-lamp, in sharp contrast to the monomeric dye in THF (Fig. 1a). In contrast, when an NDI-1 solution in THF (0.1 mg in 0.3 mL) was injected into water (2.7 mL) in the absence of any lipid, immediately a red solid precipitated out (Fig. S1†), indicating the essential role of the DSPE-PEG in producing a stable colloidal dispersion.

Dynamic light scattering (DLS) studies with SPNR-1 revealed (Fig. 1b) an average hydrodynamic diameter (D_h) of 220 nm while the aqueous dispersion of only DSPA-PEG showed a D_h of 12 nm.

The transmission electron microscopy (TEM) image (Fig. 1c) showed quite uniform nanorod morphology with lengths in a range of 170–230 nm and widths of ~40–60 nm. The relatively larger diameter of the SPNRs in DLS than their estimated length in TEM can be attributed to drying effects during TEM sample preparation.[14] DSPA-PEG alone, in contrast, showed (Fig. S2†) a spherical micellar morphology with an average diameter of ~10 nm, corroborating with the DLS result. Energy-dispersive X-ray spectroscopy (EDS) analysis on SPNR-1 revealed a strong peak of the element sulphur (Fig. S3†) confirming the presence of sulphur containing NDI-1 in the nanorod. As the cursory observation (Fig. 1a) indicated strong fluorescence, we examined the morphology of SPNR-1 by fluorescence microscopy (Fig. 1d) which showed bright red emitting nanorods similar to those observed in TEM. The size and shape of the nanomaterials often influence their cellular uptake[15] and other properties. For conjugated polymer-based nanoparticles,[7] it has been reported that the size can be tuned by varying the concentration of the polymer and/or its ratio with the lipid. To test such possibilities, we repeated a similar formulation of SPNR synthesis by lowering the amount of NDI-1 by ten times and keeping all other parameters the same, which also produced a similar fluorescent pellucid suspension (SPNR-2, Fig. 1a). DLS (Fig. 1b) showed a sharp peak with an average D_h of 51 nm suggesting the formation of significantly smaller nanorods which was confirmed by TEM (Fig. S4a†) and fluorescence microscopy (Fig. S4b†) images.

The UV/Vis spectra of SPNR-1 showed a significant bathochromically shifted (~35 nm) sharp absorption band in the window of 450–550 nm for both SPNR-1 and SPNR-2 compared to the monomeric NDI-1 in THF (Fig. 2). Such a bathochromically shifted absorption spectrum is the typical signature of J-aggregation and can be attributed to the allowed optical excitation from the ground state to the lower energy excitonic state.[16] Identical UV/Vis spectra of SPNRs in water and the supramolecular polymer of NDI-1 in decane[6] confirmed similar J-aggregation of NDI-1 in the lipid-coated confined environment in water. The fluorescence spectra of SPNR-1 or SPNR-2 in water (Fig. 2) were also identical to that of NDI-1 in decane and exhibited a typical signature of J-aggregation with a perfect mirror-image symmetry with the absorption bands and relatively small Stoke's shift of about 20 nm compared to 43 nm for the broad and weak emission bands of the monomeric dye in THF.

This is consistent with typical J-aggregation and can be attributed to the localization of the excitation energy.[16] The

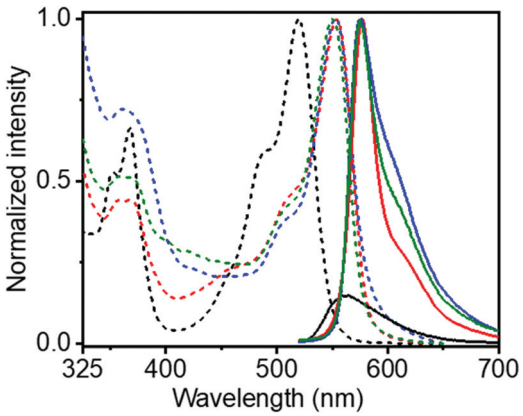

Fig. 2 Normalized absorbance (dashed lines) and emission (solid lines) spectra of NDI-1 (c = 0.35 mM) in THF (black) and decane (red), SPNR-1 (blue) and SPNR-2 (green) at 25 °C; concentration of NDI-1 = 0.34 mM and 0.031 mM in SPNR-1 and SPNR-2, respectively; λ_{ex} = 500 nm.

fluorescence quantum yields (Φ) of SPNR-1 and SPNR-2 were estimated (by an absolute method) to be 53% and 55%, respectively, while that for the monomeric NDI-1 in THF was found to be merely 0.5%, indicating a two orders of magnitude increase for the confined supramolecular polymer. The Φ values for the SPNRs were even significantly higher than those of the supramolecular polymer of NDI-1 (43%) in decane,[6] although similar J-aggregates were observed in both cases. This can be attributed to the minimized non-radiative decay in SPNRs by solvent quenching and others as the emitting supramolecular polymers, insulated by the lipid casing, are protected from the bulk solvent. Such high photoluminescence quantum efficiency has rarely been reported[17] for supramolecular assemblies of π-systems[18] and to our knowledge this is a new benchmark for supramolecular assemblies in aqueous media.

To understand the growth process of SPNRs, the UV/Vis spectra (Scheme 2a and b) of the sample were monitored during THF removal at a fixed temperature of 50 °C. Just after the injection of the mixed solution of the monomeric NDI-1 + DSPE-PEG in THF into excess water, a broad spectrum was observed with a predominant monomeric band (λ_{max} = 521 nm). However, it was neither similar to that of the monomer in THF nor the J-aggregate in the SPNRs (Scheme 2a). The intensity of the J-aggregate band (monitored at 554 nm) showed no change up to about 60 min and then increased abruptly and saturated after 90 min (Scheme 2b). The spectrum recorded after 2 h showed the appearance of a sharp bathochromically shifted absorption band confirming well-defined J-aggregation.

Based on these observations, it is proposed (Scheme 2c) that when the molecularly dissolved NDI-1 and lipid mixture in THF was injected into water, due to an abrupt change in the solvent polarity, NDI-1 formed an ill-defined colony. The hydrophobic tails of the lipid entangled with the hydrocarbon chains of such loosely bound aggregates, while the hydrophilic PEG chains remained exposed to water, preventing visible phase separation of the cluster. With gradual evaporation, when the THF concentration reached below a critical value, the onset of J-aggregation within the lipid-encased NDI-1 cluster was realized while the attached lipid molecules possibly re-oriented to encase the growing hydrophobic supramolecular polymer producing a homogeneous dispersion of SPNRs. Comparing the absorption intensity of the J-band (at λ = 554 nm) in the SPNR with that of the J-aggregated NDI-1 in decane (Fig. S5†), the encapsulation efficiency was roughly estimated to be 86% and 82%, respectively, for SPNR-1 and SPNR-2, indicating that such a formulation could be highly effective for transferring hydrophobic supramolecular polymers to biological media.

Temperature dependent UV/Vis spectra of NDI-1 in decane (Fig. 3a) showed the disappearance of the J-band and reappearance of the monomeric band at elevated temperature, indicating thermal depolymerization. In sharp contrast, J-aggregated NDI-1 in SPNR-1 did not show (Fig. 3b) any significant spectral change up to 90 °C. Even in SPNR-2 with 10-times less dye concentration, no melting was observed up to 90 °C (Fig. S6†), indicating the remarkable thermal stability of the SPNR. While such high thermal stability has been reported for selected examples of supramolecular assemblies,[19] in this particular case the noteworthy fact is that the same J-aggregate that melts at T > 60 °C in decane remains stable at least up to 90 °C when entrapped in the SPNR, which can be attributed to the confinement effect. This exceptional thermal stability of the SPNR was re-confirmed from DSC traces (Fig. 3d). NDI-1 in decane showed an endothermic peak

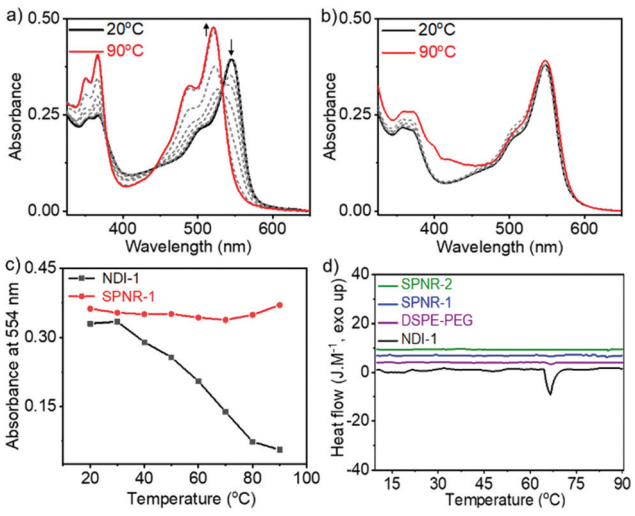

Fig. 3 Temperature dependent UV/Vis spectra (l = 0.1 cm) of (a) NDI-1 in decane (c = 0.35 mM), (b) SPNR-1 in water (concentration of NDI-1 = 0.34 mM) and (c) corresponding absorbance (at 554 nm) *vs.* temperature plot; (d) micro-DSC traces (2nd heating, *exo*-up) of SPNRs (NDI-1 concentration: 0.34 mM and 0.031 mM for SPNR-1 and SPNR-2, respectively), DSPA-PEG (c = 2.0 mg mL^{-1}) and NDI-1 in decane (c = 0.35 mM). In (b), the minor spectral changes (below 450 nm) at 90 °C possibly indicate some molecular reorganization at the elevated temperature.

(T_m = 66 °C, ΔH = 4.1 kJ mol^{-1}) due to disassembly at T > 60 °C corroborating with the melting curve from UV/Vis spectra (Fig. 3c), but no such thermal transition was observed for SPNR-1, SPNR-2 or the lipid itself. The UV/Vis spectra of SPNR-1, checked after six months, were no different from those of the freshly prepared sample (Fig. S7†) and no visible precipitation was observed during this time, indicating excellent colloidal stability. We also examined the UV/Vis spectra in the presence of 5% trifluoro-acetic acid which destroyed the J-aggregate in decane but not in the SPNR (Fig. S8†), indicating its stability under harsh acidic conditions as well.

The chirotopic properties[20] of SPNR-1 were examined by circular dichroism (CD) spectroscopy (Fig. 4a). No CD band was observed for the monomeric dye in THF, but a distinct bisignated CD spectrum was observed for SPNR-1 with a positive band at λ_{max} = 363 nm followed by a transition at relatively lower wavelength which was split into two negative bands at λ_{max} = 493 nm and 530 nm, followed by another transition and a positive band at λ_{max} = 557 nm, indicating the presence of a chiral supramolecular polymer in the SPNR. SPNR-2 also showed similar features in its CD spectrum (Fig. S9a†). An identical CD spectrum at 90 °C (Fig. 4a) confirmed the exceptional thermal stability as discussed earlier (Fig. 3).

In contrast, the CD bands of the NDI-1 supramolecular polymer in decane[21,22] disappeared (Fig. S10†) at elevated temperature, reiterating the advantage of the lipid-aided encapsulation strategy for enhanced thermodynamic stability. To check if such helicity can be probed by microscopy, the AFM image of SPNR-1 was recorded, which revealed (Fig. S11†) similar nanorod structures to those seen in the TEM and fluorescence microscopy images (Fig. 1). However, the helical structure could not be visualized which may be related to the fact that in the present system, the helical supramolecular polymers are encased by the lipid layer and the resolution of the technique does not allow the visualization of the microstructure of the encapsulated polymers.

SPNR-1 and SPNR-2 were further investigated for circularly polarized luminescence (CPL),[23] which is related to excited state chirotopic properties and they have been studied with great interest for different supramolecular assemblies in the recent past.[24,25] A prominent CPL band was observed for both SPNR-1 (Fig. 4b) and SPNR-2 (Fig. S9b†), while it was almost non-detectable for the monomeric dye in THF.[26] Similar to CD, the CPL spectra also did not show any change (Fig. 4b) at elevated temperature. From the CPL spectra, the g_{lum} (chiral dissymmetry factor) was estimated (Fig. S12a†) to be ~0.8 × 10^{-1} for both the samples which is about two times higher than that of the NDI-1 supramolecular polymer in decane.[6] Even in an absolute scale, this may be considered as an exceptionally high value and it ranks amongst the very few topmost values reported for chiral supramolecular assemblies.[25h]

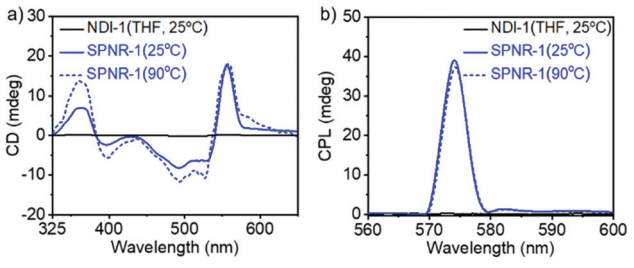

Fig. 4 (a) CD and (b) CPL spectra of NDI-1 in THF (c = 0.35 mM) and SPNR-1 in water (NDI-1 concentration = 0.34 mM; l = 0.1 cm). Molar ellipticity at λ_{max} for SPNR-1 (25 °C) was estimated to be 5.36 × 10^5 M^{-1} cm^{-1} from the CD spectrum.

Conclusions

We have demonstrated a simple and generally applicable strategy for transferring hydrophobic supramolecular polymers to the biological medium by a lipid-aided nanoprecipitation method which produces well-defined nanorods with tunable size by varying the monomer/lipid ratio. It exhibits strong impact in enhancing the thermodynamic stability, photoluminescence efficiency and chiroptical properties, all attributed to the confinement effect. While such nanomaterials derived from covalent conjugated polymers[7] or bio-molecules[27] have been studied, supramolecular polymers have not been explored. The present results open up a new paradigm for the formulation of well-defined nanostructures from supramolecular polymers of structurally diverse π-systems for elucidating their growth mechanism[3] or crystallization[28] in a confined environment and testing the scope for biological and optoelectronic applications.

Conflicts of interest

There are no conflicts to declare.

Acknowledgements

AM, DSP and HK thank the CSIR, India for a research fellowship. SG thanks the DST, Government of India for funding through the SwarnaJayanti Fellowship project (grant number: DST/SJF/CSA-01/2-14-15). SG thanks the IACS, Kolkata for generous support to create the CPL facility.

Notes and references

1 (*a*) T. F. A. De Greef, M. M. J. Smulders, M. Wolffs, A. P. H. J. Schenning, R. P. Sijbesma and E. W. Meijer, *Chem. Rev.*, 2009, **109**, 5687; (*b*) F. Würthner, C. R. Saha-Möller, B. Fimmel, S. Ogi, P. Leowanawat and D. Schmidt, *Chem. Rev.*, 2016, **116**, 962; (*c*) S. S. Babu, V. K. Praveen and A. Ajayaghosh, *Chem. Rev.*, 2014, **114**, 1973; (*d*) L. Yang, X. Tan, Z. Wang and X. Zhang, *Chem. Rev.*, 2015, **115**, 7196; (*e*) C. Rest, R. Kandanelli and G. Fernández, *Chem. Soc. Rev.*, 2015, **44**, 2543; (*f*) A. Das and S. Ghosh, *Chem.*

Commun., 2016, **52**, 6860; (*g*) S. Yagai, Y. Kitamoto, S. Datta and B. Adhikari, *Acc. Chem. Res.*, 2019, **52**, 1325; (*h*) C. Kulkarni, S. Balasubramanian and S. J. George, *ChemPhysChem*, 2013, **14**, 661.

2 (*a*) A. Saeki, Y. Koizumi, T. Aida and S. Seki, *Acc. Chem. Res.*, 2012, **45**, 1193; (*b*) V. K. Praveen, B. Vedhanarayanan, A. Mal, R. K. Mishra and A. Ajayaghosh, *Acc. Chem. Res.*, 2020, **53**, 496; (*c*) F. Würthner, *Acc. Chem. Res.*, 2016, **49**, 868.

3 (*a*) P. A. Korevaar, T. F. A. De Greef and E. W. Meijer, *Chem. Mater.*, 2014, **26**, 576; (*b*) M. Wehner and F. Würthner, *Nat. Rev. Chem.*, 2020, **4**, 38; (*c*) B. Adelizzi, N. J. V. Zee, L. N. J. de Windt, A. R. A. Palmans and E. W. Meijer, *J. Am. Chem. Soc.*, 2019, **141**, 6110; (*d*) J. Matern, Y. Dorca, L. Sánchez and G. Fernández, *Angew. Chem., Int. Ed.*, 2019, **58**, 16730; (*e*) Z. Huang, B. Qin, L. Chen, J.-F. Xu, C. F. J. Faul and X. Zhang, *Macromol. Rapid Commun.*, 2017, **38**, 1700312; (*f*) M. Hartlieb, D. H. Mans and S. Perrier, *Polym. Chem.*, 2020, **11**, 1083; (*g*) G. Ghosh, P. Dey and S. Ghosh, *Chem. Commun.*, 2020, **56**, 6757.

4 (*a*) C. Wang, Z. Wang and X. Zhang, *Acc. Chem. Res.*, 2012, **45**(4), 608; (*b*) D. Görl, X. Zhang and F. Würthner, *Angew. Chem., Int. Ed.*, 2012, **51**, 6328; (*c*) E. Krieg, M. M. C. Bastings, P. Besenius and B. Rybtchinski, *Chem. Rev.*, 2016, **116**, 2414; (*d*) M. R. Molla and S. Ghosh, *Phys. Chem. Chem. Phys.*, 2014, **16**, 26672.

5 M. J. Webber, E. A. Appel, E. W. Meijer and R. Langer, *Nat. Mater.*, 2016, **15**, 13.

6 A. Mukherjee and S. Ghosh, *Chem. – Eur. J.*, 2020, **26**, 12874.

7 J. Pecher and S. Mecking, *Chem. Rev.*, 2010, **110**, 6260.

8 (*a*) S. Wang, D. Yin, W. Wang, X. Shen, J.-J. Zhu, H.-Y. Chen and Z. Liu, *Sci. Rep.*, 2016, **6**, 22757; (*b*) P. K. Kandel, L. P. Fernando, P. C. Ackroyd and K. A. Christensen, *Nanoscale*, 2011, **3**, 1037; (*c*) L. Zhang, W. Che, Z. Yang, X. Liu, S. Liu, Z. Xie, D. Zhu, Z. Su, B. Z. Tang and M. R. Bryce, *Chem. Sci.*, 2020, **11**, 2369.

9 J. Lyklema, *Fundamentals of Interface and Colloid Science*, 1995, vol. 2, p. 3208.

10 For examples on supramolecular assembly based nanoparticles, see: (*a*) K. Li, Y. Jiang, D. Ding, X. Zhang, Y. Liu, J. Hua, Si.-S. Fenga and B. Liu, *Chem. Commun.*, 2011, **47**, 7323; (*b*) H.-Q. Peng, C.-L. Sun, L.-Y. Niu, Y.-Z. Chen, L.-Z. Wu, C.-H. Tung and Q.-Z. Yang, *Adv. Funct. Mater.*, 2016, **26**, 5483; (*c*) F.-W. Liu, L.-Y. Niu, Y. Chen, V. Ramamurthy, L.-Z. Wu, C.-H. Tung, Y.-Z. Chen and Q.-Z. Yang, *Chem. – Eur. J.*, 2016, **22**, 18132.

11 For encapsulation mediated supramolecular assembly, see: S. Sao, I. Mukherjee, P. De and D. Chaudhuri, *Chem. Commun.*, 2017, **53**, 3994.

12 For supramolecular emulsion/interfacial polymerization, see: (*a*) S. Zhang, B. Qin, Z. Huang, J.-F. Xu and Xi Zhang, *ACS Macro Lett.*, 2019, **8**(2), 177; (*b*) B. Qin, S. Zhang, Q. Song, Z. Huang, J.-F. Xu and X. Zhang, *Angew. Chem., Int. Ed.*, 2017, **56**, 7639.

13 B. García-Pinel, C. Porras-Alcalá, A. Ortega-Rodríguez, F. Sarabia, J. Prados, C. Melguizo and J. M. López-Romero, *Nanomaterials*, 2019, **9**, 1.

14 J. P. Patterson, M. P. Robin, C. Chassenieux, O. Colombani and R. K. O'Reilly, *Chem. Soc. Rev.*, 2014, **43**, 2412.

15 (*a*) S. Zhang, H. Gao and G. Bao, *ACS Nano*, 2015, **9**, 8655; (*b*) C. Huang, P. J. Butler, S. Tong, H. S. Muddana, G. Bao and S. Zhang, *Nano Lett.*, 2013, **13**, 1611.

16 For recent reviews on J-aggregation, see: (*a*) F. Würthner, T. E. Kaiser and C. R. Saha-Moller, *Angew. Chem., Int. Ed.*, 2011, **50**, 3376; (*b*) N. J. Hestand and F. C. Spano, *Chem. Rev.*, 2018, **118**, 7069.

17 T. E. Kaiser, H. Wang, V. Stepanenko and F. Würthner, *Angew. Chem., Int. Ed.*, 2007, **46**, 5541.

18 For review on fluorescent supramolecular polymers, see: (*a*) H. Wang, X. Ji, Z. Li and F. Huang, *Adv. Mater.*, 2017, **29**, 1606117; (*b*) S. S. Babu, K. K. Kartha and A. Ajayaghosh, *J. Phys. Chem. Lett.*, 2010, **1**, 3413.

19 (*a*) A. Kawasaki, T. Takeda, N. Hoshino, W. Matsuda, S. Seki and T. Akutagawa, *J. Phys. Chem. C*, 2019, **123**, 15451; (*b*) H. Abe, A. Kawasaki, T. Takeda, N. Hoshino, W. Matsuda, S. Seki and T. Akutagawa, *ACS Appl. Mater. Interfaces*, 2020, **12**, 37391.

20 (*a*) A. R. A. Palmans and E. W. Meijer, *Angew. Chem., Int. Ed.*, 2007, **46**, 8948; (*b*) P. Duan, H. Cao, L. Zhang and M. Liu, *Soft Matter*, 2014, **10**, 5428; (*c*) E. Yashima, N. Ousaka, D. Taura, K. Shimomura, T. Ikai and K. Maeda, *Chem. Rev.*, 2016, **116**, 13752.

21 Comparison of the CD spectra of SPNR-1 with that of the supramolecular polymer of NDI-1 in decane showed (Fig. S10†) not only a spectral shift but the nature and relative intensity of the bands also changed significantly. It is noteworthy that for membrane proteins such effects have been reported (ref. 22) and studied in great detail which indicate that such differences may arise due to orientational effects, difference in dielectric constants in the vicinity and so on. The observed differences may be related to these effects or even the nature of the helicity of the supramolecular polymer grown in the confined environment may be different from that in the bulk solvent which will be investigated in detail in the future.

22 A. J. Miles and B. A. Wallace, *Chem. Soc. Rev.*, 2016, **45**, 4859.

23 J. P. Riehl and F. S. Richardson, *Chem. Rev.*, 1986, **86**, 1.

24 For a review on CPL of suramolecular assemblies, see: J. Kumar, T. Nakashima and T. Kawai, *J. Phys. Chem. Lett.*, 2015, **6**, 3445.

25 (*a*) K. Ma, W. Chen, T. Jiao, X. Jin, Y. Sang, D. Yang, J. Zhou, M. Liu and P. Duan, *Chem. Sci.*, 2019, **10**, 6821; (*b*) D. Yang, P. Duan, L. Zhang and M. Liu, *Nat. Commun.*, 2017, **8**, 15727; (*c*) F. Salerno, J. A. Berrocal, A. T. Haedler, F. Zinna, E. W. Meijer and L. D. Bari, *J. Mater. Chem. C*, 2017, **5**, 3609; (*d*) Y. Wang, X. Li, F. Li, W.-Y. Sun, C. Zhu and Y. Cheng, *Chem. Commun.*, 2017, **53**, 7505; (*e*) J. Liang, P. Guo, X. Qin, X. Gao, K. Ma, X. Zhu, X. Jin, W. Xu and L. Jiang, *ACS Nano*, 2020, **14**, 3190; (*f*) R. Sethy, J. Kumar, R. Metivier, M. Louis, K. Nakatani, N. M. T. Mecheri, A. Subhakumari, K. G. Thomas, T. Kawai and T. Nakashima, *Angew. Chem., Int. Ed.*, 2017, **56**, 15053; (*g*) T. Ikeda, T. Masuda, T. Hirao, J. Yuasa, H. Tsumatori,

T. Kawaib and T. Haino, *Chem. Commun.*, 2012, **48**, 6025; (*h*) Y. Wang, Y. Jiang, X. Zhu and M. Liu, *J. Phys. Chem. Lett.*, 2019, **10**, 5861.

26 To eliminate any experimental artifacts in the CPL measurements, we have repeated the CPL experiments ten times when reproducible curves were obtained (Fig. S13†). Furthermore, the CD or CPL spectra of the lipid alone in the same solvent did not show any band (Fig. S14†) confirming a lack of any signal from the solvent or the lipid. We further checked the CPL of the standard sample, D and L-camphor (that came with the instrument) which showed the expected spectra (Fig. S15†), suggesting proper functioning of the instrument.

27 Z. Zeng, C. Dong, P. Zhao, Z. Liu, L. Liu, H.-Q. Mao, K. W. Leong, X. Gao and Y. Chen, *Adv. Healthcare Mater.*, 2019, **8**, 1801010.

28 E. C. Davidson and R. A. Segalman, *Macromolecules*, 2017, **50**, 6128.